Tectonophysics 624–625 (2014) 3–14

Contents lists available at ScienceDirect

Tectonophysics

journal homepage: www.elsevier.com/locate/tecto

Eight good reasons why the uppermost mantle could be magnetic

Eric C. Ferré [a,*], Sarah A. Friedman [a], Fatíma Martín-Hernández [b,c], Joshua M. Feinberg [d], Jessica L. Till [e], Dmitri A. Ionov [f], James A. Conder [a]

[a] Department of Geology, Southern Illinois University, Carbondale, IL 62901-4324, USA
[b] Department of Geophysics, Universidad Complutense de Madrid, Madrid 28040, Spain
[c] Instituto de Geociencias IGEO (UCM-CSIC), Fac. CC. Físicas, Av. Complutense s/n, 28040 Madrid, Spain
[d] Institute for Rock Magnetism, University of Minnesota, Minneapolis, MN 55455, USA
[e] Institut de Minéralogie et de Physique des Milieux Condensés, Paris, 75005, France
[f] Géosciences Montpellier, UMR CNRS-UM2 5243/Université Montpellier II, 34095 Montpellier Cedex 05, France

ARTICLE INFO

Article history:
Received 30 June 2013
Received in revised form 24 December 2013
Accepted 4 January 2014
Available online 16 January 2014

Keywords:
Mantle
Xenolith
Magnetization
Magnetic anomaly
Magnetite
NRM

ABSTRACT

Wasilewski et al. (1979) concluded that no magnetic remanence existed in the uppermost mantle and that even if present, such sources would be at temperatures too high to contribute to long wavelength magnetic anomalies (LWMA). However, new collections of unaltered mantle xenoliths indicate that the uppermost mantle could contain ferromagnetic minerals. 1. The analysis of some LWMA over cratons and forearcs suggest magnetic sources in the uppermost mantle. 2. The most common ferromagnetic phase in the uppermost mantle is stoichiometric magnetite. Assuming a 30 km-thick crust, and crustal and mantle geotherms of 15 °C/km and 5 °C/km, respectively, the 600 °C Curie temperature implies a 30 km-thick layer of mantle. 3. The uppermost mantle is cooler than 600 °C in Archean and Proterozoic shields (>350 °C), subduction zones (>300 °C) and old oceanic basins (>250 °C). 4. Recently investigated sets of unaltered mantle xenoliths contain pure magnetite inclusions in olivine and pyroxene formed in equilibrium with the host silicate. 5. The ascent of mantle xenoliths occurs in less than a day. Diffusion rates in olivine suggest that the growth of magnetite possible within this time frame cannot account for the size and distribution of magnetite particles in our samples. 6. Demagnetization of natural remanent magnetization (NRM) of unaltered mantle xenoliths unambiguously indicates only a single component acquired upon cooling at the Earth's surface. This is most easily explained as a thermoremanent magnetization acquired by pre-existing ferromagnetic minerals as xenoliths cool rapidly at the Earth's surface from magmatic temperatures, acquired during ascent. 7. Modern experimental data suggest that the wüstite–magnetite oxygen buffer and the fayalite–magnetite–quartz oxygen buffer extend several tens of km within the uppermost mantle. 8. The magnetic properties of mantle xenoliths vary consistently across tectonic settings. In conclusion, the model of a uniformly non-magnetic mantle should be revisited.

© 2014 Elsevier B.V. All rights reserved.

1. Introduction

A common assumption underlying the inversion of long wavelength magnetic anomalies (LWMA) is that the mantle does not contribute (Warner and Wasilewski, 1995; Wasilewski, 1987; Wasilewski and Mayhew, 1992; Wasilewski et al., 1979). Here, we challenge this view for eight major reasons and explain why this paradigm may not apply globally. Of the 400 xenoliths measured by Wasilewski and coworkers, magnetic remanence is available for 131 specimens only. This Wasilewski collection includes garnet peridotites and eclogites, i.e., mantle rocks that would not be cold enough to carry a magnetic remanence at mantle depths. Thirty percent of the Wasilewski collection consists of volumetrically minor components of the lithospheric mantle such as wehrlites. Among the remaining samples, thirty percent display macroscopically visible alteration (e.g., #110597; Wasilewski et al., 1979) and approximately twenty percent show contamination by host basalt (e.g., #ANT50; Warner and Wasilewski, 1995). Of the 26 remaining unaltered and uncontaminated samples, surprisingly little rock magnetic data is reported. Saturation magnetization (M_s) was reported for 22 samples, while magnetic susceptibility (K) was reported for only 11 samples. This small dataset shows a large variability (M_s ranges over 3 orders of magnitude, and K by a factor of ~40. The existing dataset is also overrepresented by xenoliths from Western USA (~40%). Some of the specimens show microstructural evidence of incipient partial melting at olivine–chromite grain boundaries (Warner and Wasilewski, 1995). Finally, the depth and temperature of equilibration associated with each xenolith remain unknown. Wasilewski et al. concluded that 1) magnetite constitutes the main magnetic remanence carrier, although a few xenoliths host pyrrhotite and/or native iron and 2) the lithospheric mantle is too weakly magnetic and too hot to contribute to magnetic anomalies.

* Corresponding author.
E-mail address: eferre@geo.siu.edu (E.C. Ferré).

0040-1951/$ – see front matter © 2014 Elsevier B.V. All rights reserved.
http://dx.doi.org/10.1016/j.tecto.2014.01.004

2. Reason 1. Mantle contribution to LWMA deduced from satellite data

The origin of LWMA has long been debated (e.g., Dunlop et al., 2010; McEnroe and Brown, 2000; Shive, 1989). For some (e.g., Shive, 1989; Williams et al., 1985), and the magnetizations measured in lower crust rocks are too weak to account for the observed magnetic anomalies. This "missing magnetization" stimulated a quest for strongly magnetized lower crust rocks. For others, there is no missing magnetization when magnetizations measured from rocks are properly reconciled with magnetization computed from magnetic anomalies (e.g., Ravat, 2012).

We propose an alternative hypothesis that additional magnetization could, in some regions, reside in the lithospheric mantle. If this is true, then deep crustal rocks do not need to be as strongly magnetized as previously thought and the Moho should not be considered an absolute magnetic boundary. Up to now this idea has been rejected based on the conclusions of Wasilewski et al. (1979) and Wasilewski and Mayhew (1992) that mantle rocks are too weakly magnetic and too hot to contribute to LWMA. This view, however, is increasingly at odds with a growing number of studies suggesting that the source of some LWMA lies in the lithospheric mantle (Fig. 1): for example, in oceanic basins such as the Ligurian Sea (Chiozzi et al., 2005), the Caribbean Sea (Arnaiz-Rodriguez and Orihuela, 2013; Counil et al., 1989; Guevara et al., 2013), in the forearc mantle such as the Cascadia arc (Blakely et al., 2005; Bostock et al., 2002) and other oceanic regions (Arkani-Hamed, 1993; Arkani-Hamed and Strangway, 1986, 1987; Bronner et al., 2011; Dyment et al., 1997; Harrison and Carle, 1981; Popov et al., 2011; Ravat et al., 2011). In several cold geotherm areas, such as the Amsaga belt in the West Africa Craton or the Bangui region in the Central Africa Craton, magnetization may extend into the lithospheric mantle (Hemant and Maus, 2005a, 2005b; Kochemasov and Chuprov, 1990). Overall, mantle contributions to magnetic anomalies, at least in some regions, are acknowledged to be likely (e.g., Purucker and Clark, 2011; Thébault et al., 2010). In addition, the European Space Agency plans to launch in November 2013 the *Swarm* constellation of three satellites with the objective of resolving the lithospheric magnetic field with an unprecedented accuracy (Maus et al., 2006). This mission will bridge the spectral gap between satellite and airborne/marine magnetic surveys, making this proposal highly relevant to understanding the magnetic contribution of the lithospheric mantle to the overall magnetic signature observed from orbit.

3. Reason 2. Magnetic minerals in upper mantle rocks

The upper mantle consists mainly of lherzolites, harzburgites and dunites, and accessorily of pyroxenites, wehrlites and eclogites (e.g., Jackson, 1998).In continental areas, the lithospheric mantle (consisting of plagioclase- and spinel-peridotites) is below the Curie temperature (T_c)[1] and can contribute to magnetic anomalies, whereas garnet-lherzolites, present at greater depths, are too hot to carry a magnetic remanence. Mantle peridotites are found at the Earth's surface either as ophiolite (e.g., Nicolas, 1986), as Alpine-type peridotites (e.g., Liou et al., 2007), or as xenoliths (e.g., Nixon, 1987). Exposed mantle rocks alter through serpentinization, a process that forms abundant magnetite (e.g., Alt and Shanks, 2003; Borradaile and Lagroix, 2001; Frost et al., 2013; Toft et al., 1990). Even weakly altered massifs are serpentinized (Christensen, 1971; Ferré et al., 2005; Le Roux et al., 2007).

Mantle xenoliths, due to their rapid ascent, provide the most pristine samples of the lithospheric mantle (Carlson, 2007; Haggerty and Sautter, 1990; Nixon, 1987). Inclusions of iron-rich phases, such as magnetite and ilmenite, may form in olivine and pyroxene at mantle conditions (e.g., Sen and Jones, 1988), during xenolith ascent, or by a combination of crack healing and metasomatism (Drury and van Roermund, 1989; Hervig, 1989; Neal et al., 2001). Also, xenoliths may be contaminated by the host magma during ascent by grain boundary

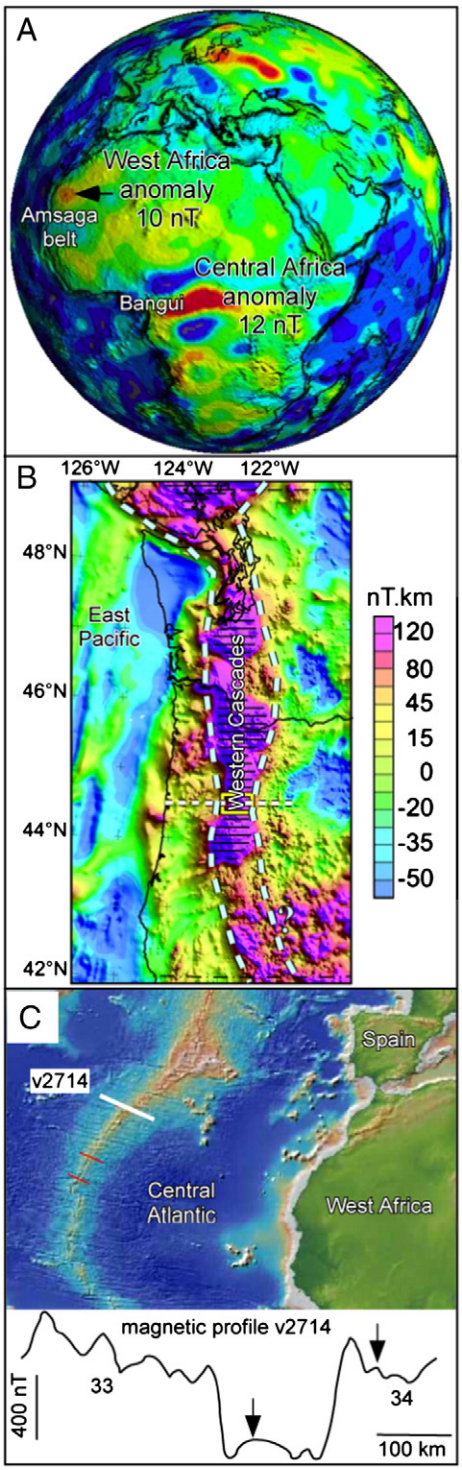

Fig. 1. The analysis of magnetic anomalies suggests the presence of magnetic sources in the upper mantle over both continental and oceanic areas such as: A. The Bangui anomaly in the Central African Craton (Kochemasov and Chuprov, 1990; Ouabego et al., 2013) and the Amsaga anomaly in the West African craton (Hemant and Maus, 2005a, 2005b); B. The Cascadia subduction zone (Blakely et al., 2005); and C. Domains of serpentinized oceanic lithosphere (Dyment et al., 1997).

[1] The temperature above which ferromagnetic minerals lose their magnetic ordering and become paramagnetic.

percolation. Finally, supergene alteration can form hematite or serpentine along grain boundaries. If care is taken when selecting samples, many of these secondary effects can be avoided. Thus, if mantle xenoliths can be shown to be relatively unaffected by these processes, they represent the best available samples to examine upper mantle magnetic mineralogy.

It is critical to this study to discern *primary* mineral assemblages formed in equilibrium at mantle depth from *secondary* assemblages formed during ascent, emplacement and subsequent alteration. We examine mantle xenoliths from the serpentinized cratonic mantle (Facer et al., 2009) and from the forearc mantle (*Kamchatka* samples).

Magnetic anomalies arise from variations in induced and remanent magnetizations held by adjacent rocks. The induced magnetization of a rock is the sum of the magnetizations of its minerals. The induced magnetization of a mineral is proportional to the mineral's magnetic susceptibility (K) and to the applied field. Table 1 summarizes the magnetic susceptibility at 300 K ($K_{300\ K}$) and saturation magnetization (M_s) of common mantle minerals. Silicate minerals, such as olivine, pyroxene and garnet, are abundant in the upper mantle, however the remanent magnetization of a peridotite arises from minor phases such as Fe-oxides, FeNi-alloys and some Fe-sulfides that show ferromagnetic behavior. Ferromagnetic minerals carry a spontaneous magnetization below T_c, and even when present at the trace concentrations, these phases have profound effects on a rock's magnetization. The presence and concentration of ferromagnetic minerals in mantle rocks are at present relatively unknown.

Several magnetic minerals may influence the magnetization of the upper mantle. Cr-spinels are common in upper mantle peridotites (e.g., Haggerty, 1995; Irvine, 1965, 1967). Chromite, often cited as a remanent phase, often owes its magnetization to magnetite inclusions (e.g., Kądziałko-Hofmokl et al., 2008; Rais et al., 1997, 2003; Thompson and Robinson, 1975). In fact, pure chromite is paramagnetic above 70 K (Derbyshire and Yearian, 1958; Gattacceca et al., 2011). Cr-spinel is ferrimagnetic only if Al + Mg < 0.2 and Fe > 0.3 (Yu and Tikoff, 2010; Ziemniak and Castelli, 2003), compositions that are uncommon in mantle peridotites. Also, ferrimagnetic Cr-spinels show a lower Curie temperature than that of magnetite, further reducing their potential contribution to remanent magnetization of mantle rocks. Our preliminary results (Section 4) show that, even in the Montferrier specimens that host 600 ppm of sulfur (Alard et al., 2011), the contribution of pyrrhotite and monosulfide solid solution to magnetic remanence is always *negligible* compared to that of magnetite. In addition, the low T_c (593 K) and low concentration of pyrrhotite prevents it from being a major contributor to magnetic remanence. FeNi alloys, such as awaruite, are stable only in very reduced conditions, FMQ −6 or −7, typically in serpentinized ultramafic rocks (Frost, 1985). The potential contribution of these alloys to magnetic remanence, despite their high T_c, ought to be negligible because these phases are rare and occur only in trace amounts. Our preliminary results further suggest that magnetite occurs systematically, albeit in variable amounts, and dominates the remanent magnetization of mantle xenoliths.

Pure (stoichiometric) magnetite has been reported in mantle xenoliths in several studies (e.g., Callahan, 2009; Ferré et al., 2013; Warner and Wasilewski, 1995; Wasilewski and Mayhew, 1992; Wasilewski et al., 1979). The origin of this magnetite (Fig. 2) is crucial to the evaluation of the magnetic properties of the lithospheric mantle, as it has to be demonstrated that it formed under mantle conditions. In general, Cr-rich spinel occurs as a primary phase in mantle peridotites formed at mantle depths (e.g., Ballhaus et al., 1991; Barnes, 2001; Ionov, 2010; Ionov et al., 2010). As the Cr content of spinel increases, it is stabilized at increasing depths in the mantle and coexists with garnet (MacGregor, 1970, 1974; Neal and Nixon, 1985). In contrast, magnetite generally forms as a secondary phase (Hwang et al., 2008; Janecky and Seyfried, 1986; Nazarova, 1994; Toft et al., 1990; Zhang et al.,

Table 1
Magnetic properties of selected minerals in mantle peridotites.

	Mineral	Formula	Magnetic order at 300 K	$K_{300\ K}$ [SI]	M_s Am²/kg	Curie T Kelvin	Reference
	Plagioclase	$(Na,Ca)(Si,Al)_4O_8$	Diamagnetic	-16×10^{-6}	–	–	Bleil and Peterson (1982)
Olivines	Forsterite	Mg_2SiO_4	Diamagnetic	-2.2×10^{-6}	–	–	Belley et al. (2009)
	Fayalite	Fe_2SiO_4	Paramagnetic	4831×10^{-6}	–	–	Belley et al. (2009)
	Olivine — Fo_{92}	$(Fe_{0.08}, Mg_{0.92})_2\ SiO_4$	Paramagnetic	517×10^{-6}	–	–	Belley et al. (2009)
Pyroxenes	Enstatite	$Mg_2Si_2O_6$	Diamagnetic	-2.2×10^{-6}	–	–	Calculation based on Syono (1960)
	Diopside	$CaMgSi_2O_6$	Diamagnetic	-2.2×10^{-6}	–	–	Calculation based on Syono (1960)
	Clinoenstatite	$Mg_2Si_2O_6$	Diamagnetic	-2.2×10^{-6}	–	–	Calculation based on Syono (1960)
	Ferrosilite	$Fe_2Si_2O_6$	Paramagnetic	2834×10^{-6}	–	–	Calculation based on Syono (1960)
	Clinoferrosilite	$Fe_2Si_2O_6$	Paramagnetic	2834×10^{-6}	–	–	Calculation based on Syono (1960)
	Hedenbergite	$CaFeSi_2O_6$	Paramagnetic	1499×10^{-6}	–	–	Calculation based on Syono (1960)
	Orthopyroxene	$(Fe_x, Mg_{2-x})Si_2O_6$	Paramagnetic	322×10^{-6}	–	–	Average of 77 Opx chemical analyses
	Clinopyroxene	$(Fe_x, Mg_{2-(x+y)}, Ca_y)Si_2O_6$	Paramagnetic	166×10^{-6}	–	–	Average of 78 Cpx chemical analyses
Fe-rich minerals	Ilmenite	$FeTiO_3$	Antiferromagnetic	$4.7–5.2 \times 10^{-3}$	–	40	Dunlop and Özdemir (2009)
	Ulvöspinel	Fe_2TiO_4	Antiferromagnetic	4.8×10^{-3}	–	120	Dunlop and Özdemir (2009)
	Chromite (magnetite)	$(Fe_{3-x}Cr_x)O_4$	Ferrimagnetic	0.0 — 3.0	0–92	70–853	Tarling and Hrouda (1993), Gattacceca et al. (2011)
	Pure chromite	$FeCr_2O_4$	Ferrimagnetic	530×10^{-6}	16	70	Dahlin and Rule (1993), Gattacceca et al. (2011)
	Pure magnetite	αFe_3O_4	Ferrimagnetic	3.0	92	853	Dunlop and Özdemir (1997)
	Titanomagnetite	$(Fe_{3-x}Ti_x)O_4$	Ferrimagnetic	0.13–0.62	0–92	120–853	Dunlop and Özdemir (2009)
	Maghemite	γFe_2O_3	Ferrimagnetic	2.0–2.5	74	953	Dunlop and Özdemir (1997)
	Pyrrhotite	Fe_7S_8	Ferrimagnetic	3.2**–49 $\times 10^{-3}$	17	593***	Dekkers (1988), Dunlop and Özdemir (2009)
	Native iron	αFe	Ferrimagnetic	3.9	218	1038	Dunlop and Özdemir (2009)
	Josephinite	$FeNi_3$	Ferrimagnetic	>1.0	120	883	Wasilewski (1988)
	Wairauite	CoFe	Ferrimagnetic	>1.0	235	1241	Moskowitz (1991)
	Garnet	$(Fe,Mg)_3Al_2(SiO_4)_3$	Paramagnetic	398×10^{-6}	–	–	Average of 112 chemical analyses (pyrope)
	Serpentine	$((Mg, Fe)_3Si_2O_5(OH)_4)$	Paramagnetic	37×10^{-6}*	–	–	Median of 26 single crystals

* Median of paramagnetic susceptibility of 26 crystals of crysotile, lizardite, & antigorite measured at 1.7 T (to remove contribution of ferrimagnetic inclusions).
** 3.2 [SI] for Fe7S8 & 0.17 for Fe9S10; Dunlop and Özdemir (2009). 49 $\times 10^{-3}$ to 0.34 [SI] depending on grain size (Dekkers, 1988).
*** Monoclinic pyrrohotite has a Curie temperature less than 623 K & hexagonal pyrrhotite is thermally unstable with a lambda transition centered at 523 K. All ferrimagnetic pyrrhotite compositions become metastable above ≈ 523 K, therefore the Fe(1 − x)S phases should all be non magnetic at mantle temperatures.

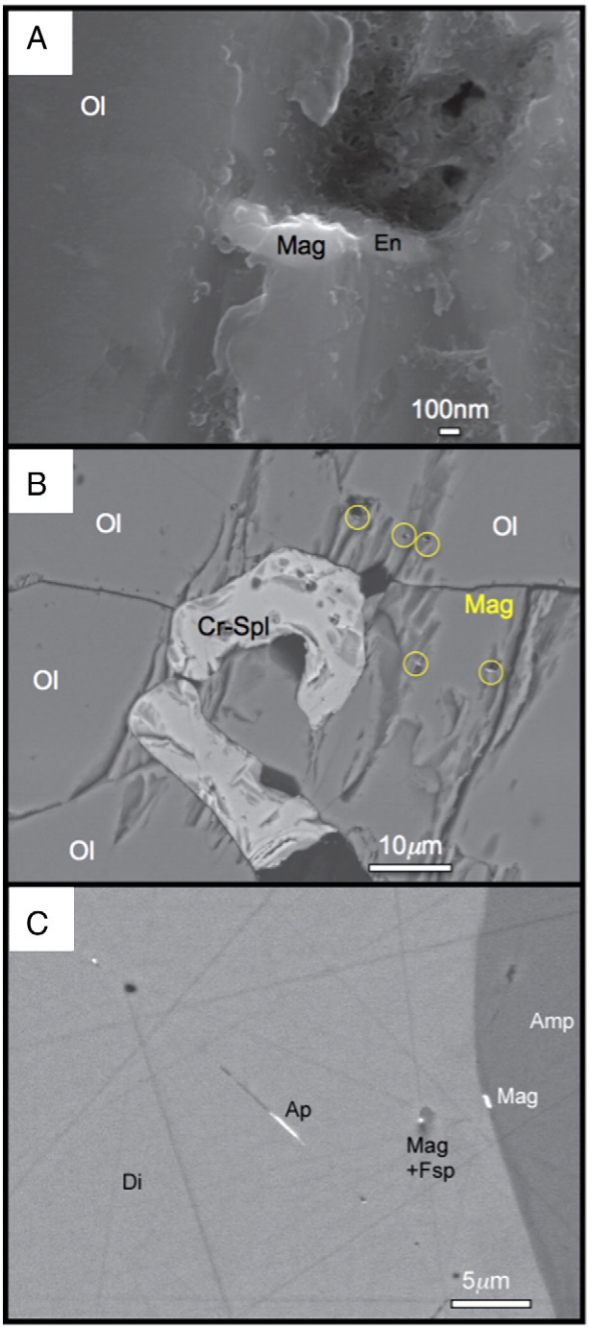

Fig. 2. Scanning electron microscope images of thin sections of a harzburgite xenolith from Avacha andesitic volcano, Kamchatka island arc (Ferré et al., 2013). A. The rock is free of post-eruptive alteration along grain boundaries. Olivine (Ol) grains host 200 nm × 500 nm, needle-shaped magnetite (Mag) inclusions adjacent to orthopyroxene (En) lamellae. B. Elongate magnetite inclusions display a lattice-controlled orientation within olivine. C. Magnetite platelets or needles 10 to 20 μm in length occur within primary olivine.

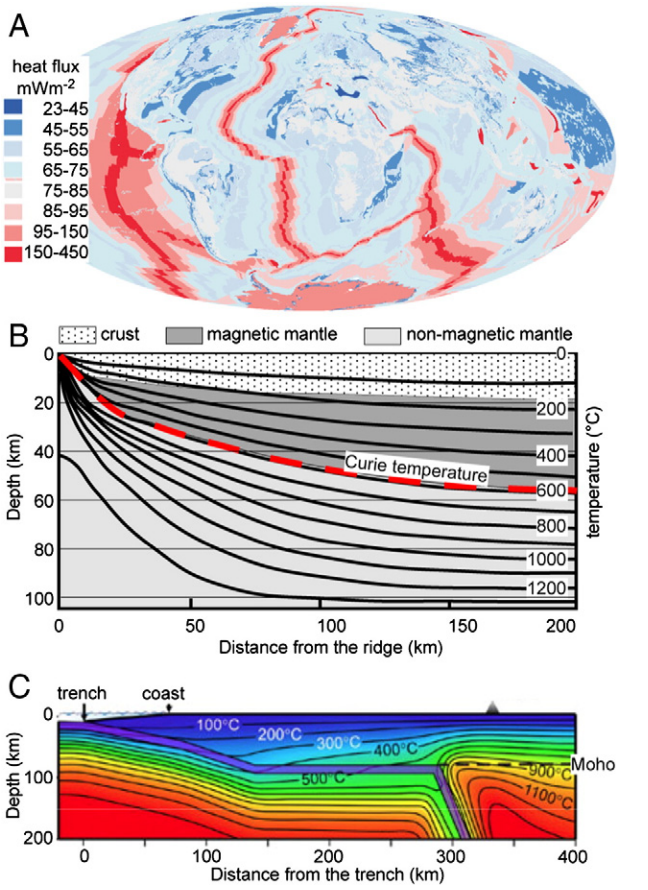

Fig. 3. The uppermost mantle can be significantly cooler than 600 °C in tectonic settings such as: A. Archean–Proterozoic shields, >350 °C (Davies and Davies, 2010); B. Old oceanic basins, >250 °C (McKenzie et al., 2005); and C. Subduction zones, >300 °C (Manea et al., 2012).

1999) resulting from interaction with oxidizing fluids or melts through one or more magnetization processes (Section 7).

4. Reason 3. Temperature of the uppermost mantle in cold geotherm regions

Temperature distribution in the lithosphere (Fig. 3) can be evaluated by i) the pressure–temperature of equilibration of mantle xenolith suites (e.g., Goncharov et al., 2012); ii) surface heat flow measurements, iii) magnetization contrasts inferred from satellite magnetic data (e.g., Manea et al., 2012), and iv) spectral magnetic depth determination of near-surface magnetic data. The xenolith-based approach, however does not inform about it on the current geotherm present in the region of origin of the xenoliths (e.g., Kobussen et al., 2008). The other approaches, combined with seismic data, have yielded realistic models for the thermal state of oceanic and continental lithospheres (e.g., Abercrombie and Ekström, 2001; McKenzie et al., 2005). Clearly, parts of the lithospheric mantle can be *cooler* than the pressure-corrected Curie temperature of magnetite (<600 ºC), for example, in cratonic interiors (e.g.; Batumike et al., 2009; Blackwell et al., 2011; Goncharov et al., 2012; Griffin et al., 2011; Jones et al., 2003), subduction zones (e.g., Bostock et al., 2002; Ernst, 1988; Liou, 1999; Tsujimori et al., 2006), and old oceanic lithosphere (e.g., Ildefonse, 2010). The geothermal gradient in the continental crust varies greatly with the age of the crust while the geothermal gradient in the upper mantle is less variable.

5. Reason 4. Magnetic properties of fresh mantle xenoliths

All xenolith specimens produce major hysteresis loops demonstrating the presence of at least one ferromagnetic sensu lato phase (Ferré et al., 2013; Friedman, 2011). This ferromagnetic contribution varies between 1 and 70% of the bulk magnetic susceptibility with an average of 21% (Ferré et al., 2013; Supplementary Data).

Some minerals, occasionally reported as carrying magnetic remanence, actually do not. For example, Cr-rich spinel behaves ferromagnetically only within a specific compositional range (Schmidbauer, 1983), and in these mantle xenoliths, previous petrological studies have shown that the iron content of Cr-rich spinel is too low to carry a magnetic remanence. Iron–nickel sulfides, such as pentlandite, cannot contribute to remanence because they are paramagnetic at

and above room temperature (Knop et al., 1976). The lack of a pyrrhotite transition around 30–34 K (Rochette et al., 1990) in low-temperature (LT) magnetic experiments, even in the Massif Central specimens, which have the highest sulfur content in mantle peridotites (≈600 ppm; Alard et al., 2011), shows that the contribution of pyrrhotite to remanence is negligible. Finally, we find no evidence for Fe–Ni alloys using either electron microscopy or rock magnetic measurements.

Pure magnetite is the ferromagnetic mineral most commonly observed in mantle xenoliths. In measurements of room temperature saturation isothermal remanent magnetization (RT-SIRM) on cooling from 300 K to 10 K, xenoliths from Hawai'i, Massif Central, Kamchatka and Siberia showed $\delta M/\delta T$ maxima at 120–125 K (Ferré et al., 2013), which corresponds to the Verwey transition of pure magnetite (e.g., Walz, 2002). This data, along with the electron microscopy results and alternating field demagnetization spectra of NRM (Supplementary Data), indicate that magnetite constitutes the dominant NRM carrier. The xenoliths' hysteresis properties (Ferré et al., 2013) are consistent with pseudo-single domain (PSD) to single domain (SD) grain sizes for this magnetite. Two samples from the Siberian craton (U503 and U504) also displayed clear pyrrhotite transitions around 30–34 K in the low temperature cycling experiments. The magnetic properties of mantle xenoliths from the United States interior are described in Friedman et al. (2014–this issue). Thus, although magnetite may be the most frequently observed ferromagnetic mineral in mantle xenoliths, pyrrhotite may also occur on a less frequent basis. However, its comparatively low Curie temperature of 320 °C makes it unlikely that pyrrhotite can contribute to either an induced or remanent magnetization in the lithospheric mantle.

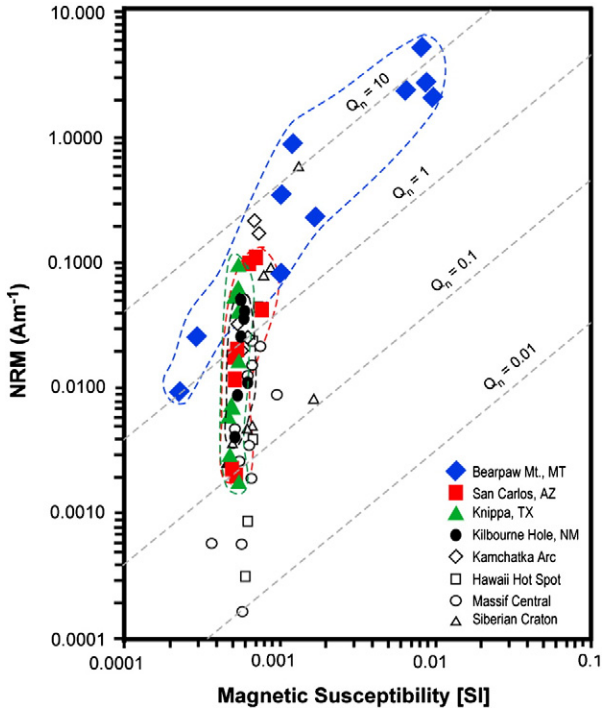

Fig. 4. Natural remanent magnetization (NRM in Am^{-1}) versus total low-field magnetic susceptibility (K_m, dimensionless in SI units) of peridotite xenoliths (details in Appendix A; full dataset in Supplemetary data). Koenigsberger ratio, $Q_n = NRM/K_mH$ where H: local geomagnetic field intensity = 40 Am^{-1}. Each suite shows a relatively narrow range of magnetic susceptibilities and a broad range of NRM values (see also Friedman et al., 2014–this issue).

6. Reason 5. Ascent of mantle xenoliths and implications for magnetic assemblages

In mantle peridotites, magnetite is commonly thought to form as a secondary phase through serpentinization at various depths: in the mantle (e.g., Facer et al., 2009), at intermediate depths (e.g., Deschamps et al., 2010), or near the surface (e.g., Malvoisin et al., 2012; Toft et al., 1990). However, in this study we argue that magnetite can form via diffusive exsolution at mantle depths within both olivine and pyroxene, or along primary silicate grain boundaries (Figs. 2; 5). Our strongest evidence for such a claim are magnetite inclusions exsolved in olivine (and frequently associated with orthopyroxene) in xenoliths from Kamchatka. These inclusions are similar to those described by Markl et al. (2001), who proposed a formational mechanism associated with a late stage rise in fO_2 conditions. Indeed, spinel grains in the Kamchatka xenoliths show an increase in Fe^{3+} from core to rim, consistent with an increase in fO_2 due to exposure to late-stage, subduction-related fluids (Goncharov et al., 2012; Ionov, 2010). Such oxidizing fluids can be present at mantle depths and may explain the magnetite observed in the other xenolith suites. In the Hawai'i xenoliths, a portion of the magnetite grains are spatially associated with amphibole lamellae, in striking similarity with the inclusions described in gabbroic olivines altered at high temperature by oceanic hydrous fluids (Puga et al., 1999). Similarly, in the Massif Central xenoliths, the amphibole lamellae exsolved along crystallographic planes within the host diopside suggests the availability of H_2O during exsolution. Our sample selection criteria exclude almost all cases of xenolith serpentinization, but when rare serpentine veins were observed, they do not host magnetite or metal alloys, but only non-ferromagnetic nickel sulfides.

The magnetite exsolution observed in this study is thought to occur during oxidation, at temperatures higher than 600 °C, and has been previously studied in pyroxene (e.g., Fleet et al., 1980; Schlinger and Veblen, 1989) and in olivine (Franz and Wirth, 2000; Kohlstedt et al., 1976; Markl et al., 2001; Putnis, 1979). In olivine, these exsolved grains tend to display both needle-like and dendritic morphologies and display high coercivities (Brewster and O'Reilly, 1988). In mantle xenoliths from a seamount, Franz and Wirth (2000) attributed the olivine oxidation event responsible for magnetite exsolution to a 700–800 °C metasomatic fluid. The exsolved magnetite observed in this study occurs within primary silicates, away from serpentine veins, and is

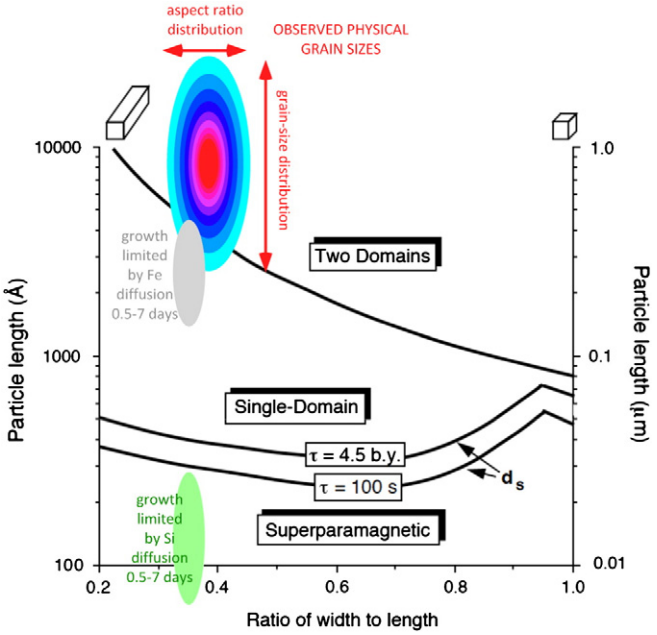

Fig. 5. The ascent of mantle xenoliths in volcanic conduits through cratons and subduction zones occurs typically in less than a day (Table 2). Our numerical models show that magnetite should not grow to sizes as large as those observed in the samples within this time frame.

consistent with formation at mantle depths or during the initial stages of ascent.

External oxidation of olivine proceeds by diffusion of Fe to grain surfaces or high-energy sites such as subgrain boundaries or dislocations, with the O and Si remaining relatively immobile in the olivine lattice (e.g., Chakraborty, 1997; Mackwell, 1992). Fe-oxides can be produced in a matter of hours by this mechanism, but its formation is highly localized at high-energy sites. No such association of oxides with grain boundaries was noted, so growth of magnetite by external oxidation of olivine during ascent is unlikely to be the source of magnetite in our samples. We also note that at high temperatures (900–1200 °C), Fo_{90} is stable at oxygen fugacities up to 4 log units above QFM (Nitsan, 1974), so an entraining basaltic melt would need to be more oxidizing than QFM + 4 to produce magnetite and pyroxene from Fo_{90} during xenolith ascent. Oxygen fugacities in MORB are typically much lower than this (Fig. 7). Alternatively, an exsolution-like breakdown of olivine can take place to produce magnetite and pyroxene, which often results in symplectic intergrowths (Moseley, 1984). This occurs without the addition of oxygen, although the reaction can be accompanied by a transformation of Fe^{2+} to Fe^{3+} if diffusion of electrons and excess Fe^{2+} out of the grain also occurs (Ashworth and Chambers, 2000). This type of reaction requires a small amount of lattice reorganization and short-range diffusion of Si away from the area occupied by the magnetite (Moseley, 1984). Measurements of Si diffusivity in olivine under hydrous conditions by Costa and Chakraborty (2008) indicate that the characteristic length scale of Si diffusion on the short time scales of xenolith ascent (Demouchy et al., 2006; Peslier et al., 2008) is too short to allow growth of the magnetite particles observed in our samples (Table 2).

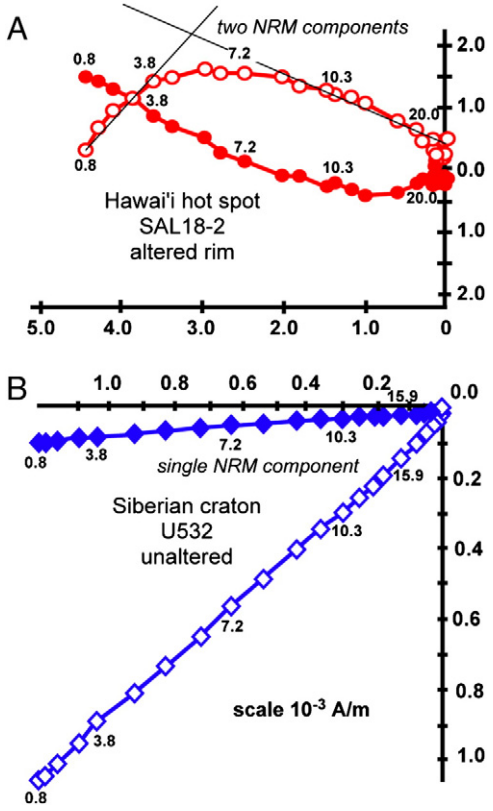

Fig. 6. Paleomagnetic analysis assists in detecting incipient xenolith alteration. AF demagnetization of natural remanent magnetization (NRM) shows that altered specimens carry multiple NRM components (A) whereas unaltered specimens always display a single NRM component (B).

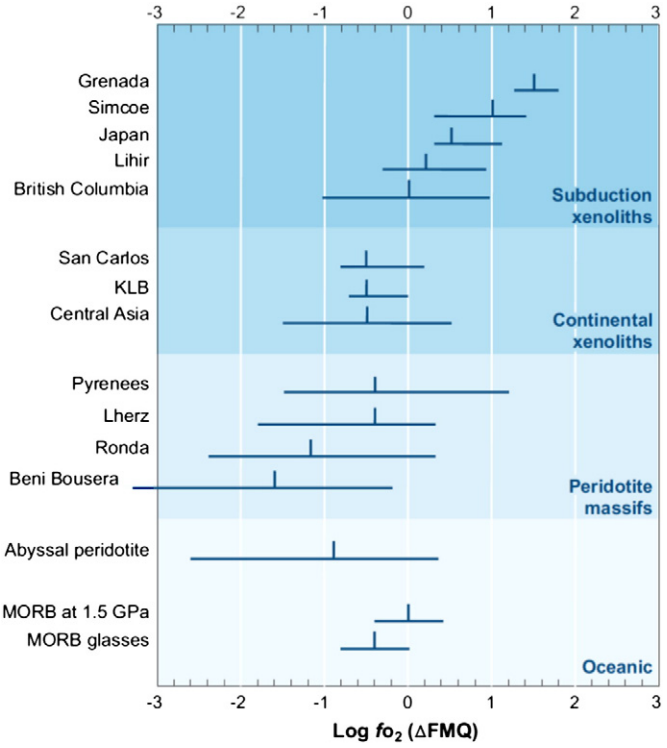

Fig. 7. Oxygen fugacities for spinel peridotites from various tectonic settings (Frost and McCammon, 2008).

7. Reason 6. Magnetization processes of mantle xenoliths and implications for mantle magnetization

7.1. Weathering

This process is caused by meteoric fluids after eruption of the host magma. In this case, the Ti-poor magnetite commonly occurs with maghemite, hematite and goethite, a mineral assemblage characteristic of supergene alteration of peridotites that gives the rock an olive green to ochre color depending on the degree of weathering (e.g., Li et al., 2008; Luguet and Lorand, 1998). Magnetically remanent phases formed after eruption often record slightly different magnetization directions (Fig. 6), which can be used to distinguish them from phases formed through oxidation at higher temperature.

7.2. Interaction with volcanic fluids and melts during ascent

The transport of mantle xenoliths from the source region to the Earth's surface involves high-temperature interaction with volcanic

Table 2
Calculated magnetite growth in olivine during xenolith exhumation.

Characteristic Fe diffusion distance, $x = 2\sqrt{(Dt)}$*, in olivine calculated using Fe–Mg diffusivities of Dohmen and Chakraborty (2007)				
	1 h	6 h	12 h	1 day
1200 °C	0.81 μm	1.0 μm	2.8 μm	4.0 μm
1100 °C	0.45 μm	0.55 μm	1.6 μm	2.2 μm
1000 °C	0.22 μm	0.55 μm	0.78 μm	1.1 μm
Characteristic diffusion distance for Si in olivine calculated using data of Costa and Chakraborty (2008)				
	1 h	6 h	12 h	1 day
1200 °C	11 nm	27 nm	38 nm	54 nm
1100 °C	3.8 nm	9.3 nm	13 nm	19 nm
1000 °C	1.1 nm	2.7 nm	3.8 nm	5.4 nm

* D is diffusivity; t is time.

fluids and melts. If the fO_2 of the melt is sufficiently high (e.g., FMQ, Magnetite–Wüstite), the formation of magnetite could be promoted. An example of lavas having oxidation states at magnetite-wüstite or higher is in Hawai'i (e.g., Rhodes and Vollinger, 2005). There are also petrographic and mineralogic indicators of such xenolith–host melt interactions witnessed by the breakdown of pyroxene and spinel to form "spongy" rims (Fig. 2a of Taylor and Neal, 1989; Fig. 2c of Kinman and Neal, 2006). It should be noted that while all xenoliths experience heating by host magmas and decompression during their transport to the surface, only a few spinels display "spongy" rims. Some kimberlite xenoliths, equilibrated at 1300 °C and transported from depths of 80–250 km almost instantaneously, show no spongy rims on clinopyroxene, orthopyroxene, spinel, or garnet. This means that the spongy rims are a result of pre-eruption mantle metasomatism, i.e., reaction with percolating melts and fluids, not decompression, nor reaction with host magmas. During this ascent, new magnetically remanent minerals such as magnetite, maghemite, or hematite may form.

7.3. Decompression during ascent

The change in pressure from mantle to crustal depths can promote back reactions between aluminous phases that are seen as slivers of pyroxene between garnet and spinel (occasionally amphibole if volatiles are available from the host magma). Such decompression would also lead to an increase in Fe^{3+} from core to boundary in the spinel adjacent to secondary pyroxene/amphibole (e.g., Neal and Nixon, 1985; Neal et al., 2001). Using the method of Quintiliani et al. (2006) the relative change in oxidation state can be estimated based upon Fe^{3+} variability across Cr-spinel grains.

7.4. Oxidative metasomatism

The challenge is to prove that magnetite formed under mantle conditions (e.g., Hofer et al., 2009; Zhao et al., 1999) and that subsequent processes have preserved the mantle signature of this mineral. Only the topmost layer of the mantle (40–70 km depth range) in cratons and subduction zones can be magnetic considering their temperature range (Pollack and Chapman, 1977). These rocks normally have FMQ of +1 to 0 (Creighton et al., 2010; Wood et al., 1990), i.e., the mantle exists at oxidation states capable of stabilizing magnetite. It should be noted, however, that the magnesium-rich olivine–magnetite–quartz oxygen buffer (Clark, 1999), which lies above FMQ, provides a more accurate representation of magnetite actual stability in the mantle. The oxygen fugacity conditions required for the stability of stoichiometric magnetite are generally not met in the pristine uppermost mantle. The presence of magnetite in the mantle, therefore, most likely requires metasomatism by oxidized fluids. The effects of such fluids can be demonstrated through careful microanalytical characterization of peridotite samples (e.g., Facer et al., 2009).

Previous studies describe the eight suites of mantle xenoliths of Fig. 4 in detail: Bearpaw Mt. (Facer et al., 2009); San Carlos (Frey and Prinz, 1978; Irving, 1980); Knippa (Frey and Prinz, 1978; Raye et al., 2011; Young and Lee, 2009); Kilbourne Hole (Bussod and Williams, 1991; Dromgoole and Pasteris, 1987); Kamchatka Arc (Ionov, 2010; Ionov et al., 2011; Soustelle et al., 2010); Hawai'i Hot Spot (Sen and Jones, 1988); Massif Central (Alard et al., 2011; Lenoir et al., 2000); Siberian Craton (Doucet et al., 2012; Goncharov et al., 2012; Ionov et al., 2010).

In each suite, the primary ferromagnesian minerals (olivine, orthopyroxene, clinopyroxene) consistently show limited core-to-rim chemical zonation. This lack of significant zonation indicates equilibration at high temperature and shows that the assemblages observed in the xenolith suites represent in-situ mantle conditions. Also, the short duration of ascent generally calculated for mantle xenoliths, combined with the large size of our xenoliths, reduces the chances for re-equilibration of the xenolith with its host magma.

In the following we emphasize only the petrologic features specific to each suite. The Bearpaw Mountains xenoliths consist of phlogopite spinel dunite with olivine (>80%), enstatite (10–15%), phlogopite (5–10%), chrome spinel (1–2%), brown amphibole (1–2%) and antigorite (1–2%). In some specimens, olivine–olivine grain contacts display thin films of antigorite hosting small alignments of magnetite grains, whereas in other specimens, magnetite forms on the rim of chromite and in-between diopside grains (Friedman et al., 2014–this issue). The San Carlos xenoliths correspond to Cr-rich diopside dunite in which magnetite inclusions up to 5 μm in length occur in some of the olivine porphyroclasts. The Knippa xenoliths are coarse grained, equigranular, fresh spinel lherzolite free of lizardite veins. Grain boundaries are straight and show well-developed triple boundaries, occasionally with spongy rims around clinopyroxenes. Magnetite has not been observed microscopically. The Kilbourne Hole xenoliths consist of Cr-diopside spinel lherzolites and spinel harzburgites with protogranular microstructures. Spongy rims around clinopyroxenes suggest reactions during ascent. Monosulfide solid solution (pyrrhotite) and other Cu–Ni–Fe sulfides such as chalcopyrite are relatively common in these peridotites. Magnetite was not observed in these xenoliths. In the Kamchatka xenoliths, spinel grains show an increase in Fe^{3+} from core to rim, consistent with an increase in fO_2 due to exposure to late-stage, subduction-related fluids. The late-stage assemblage also contains amphibole indicating hydrous fluid compositions. In the Hawai'i xenoliths, the association of amphibole and magnetite inclusions suggests a hydrous alteration process. In the Massif Central xenoliths, the presence of amphibole lamellae formed along crystallographic planes within the host diopside suggests the availability of H_2O during reaction. In this case, the platelet and needle-shaped Cr-rich spinel inclusions formed as a result of solid-state reactions, while needle-shaped magnetite inclusions formed through fluid and/or melt infiltration at ~600 °C. Thus, the magnetite observed in this study must have formed between ~350 and ~600 °C. In the Siberian xenoliths, magnetite was not observed in the very rare serpentinite veins.

7.5. Multi-stage magnetization history

The petrological evolution of mantle xenoliths outlined in the previous section corresponds to the following multi-stage magnetization history: (1) when the peridotite is formed at mantle depth, the mantle is above T_c and therefore cannot carry a remanent magnetization; (2) as the mantle cools below T_c over time, the peridotite acquires a thermoremanent magnetization (TRM_1); (3) leading up to a volcanic eruption, a hot melt comes from below, extracts the xenolith and transports it to the Earth's surface, at that point TRM_1 is completely erased because all melts (basaltic and kimberlitic) are at temperatures much higher than T_c; (4) after eruption, the xenolith cools down below T_c and acquires a new thermoremanent magnetization TRM_2; (5) if the xenolith is chemically altered, then a chemical remanent magnetization (CRM_1) is superimposed and potentially modifies TRM_2 (CRM_1 is generally carried by hematite and goethite and displays a magnetization direction distinct from TRM_1). It should be noted that in principle, alteration or oxidation during ascent may affect the mineral assemblage but cannot impart a specific CRM because it would occur mainly above T_c. Hence, specimens that have more than one directional component of magnetization are believed altered and will not be included in the magnetic database.

8. Reason 7. Oxygen fugacity and stability of magnetite in the uppermost mantle

The extent of induced and remanent magnetization in the mantle is intimately linked to the variation of fO_2 (e.g., Frost and Shive, 1989; Toft and Haggerty, 1988). fO_2 in the lithospheric mantle was first assessed using the spinel–orthopyroxene–olivine oxybarometer on spinel peridotite xenoliths (e.g., Ballhaus et al., 1990, 1991; Mattioli and Wood,

1986; Wood, 1991). Typically, fO_2 ranges from −2 to +1 relative to the fayalite–magnetite–quartz (FMQ) buffer, is heterogeneous, and tends to decrease with depth (Fig. 7). The highest fO_2 values are measured in arc-related mantle. Within cratons, fO_2 is controlled by iron equilibria involving spinel and garnet (McCammon and Kopylova, 2004). In some cratons, fO_2 increases with depth across the spinel to spinel–garnet transition, but generally remains above the stability field of native iron down to the bottom of the lithosphere (Woodland and Koch, 2003). Hence any part of the mantle having fO_2 higher than the wüstite–magnetite (WM) buffer, could potentially host magnetite. Partial melting of the mantle redistributes Fe^{3+}, producing reduced residues and oxidized magmas (e.g., Foley, 2011). Lithospheric mantle fO_2 may vary with tectonic setting, and thus its magnetic mineralogy may not be as uniform as typically assumed. In rare instances, Fe–Ni metals and sulfides may contribute to the NRM of mantle rocks (e.g., Toft and Haggerty, 1988). For example, Ishimaru et al. (2009) reported micrometer-scale native iron inclusions in mantle xenoliths from Kamchatka. However, these native metals are likely not representative of pervasive fO_2 conditions in the lithospheric mantle (especially as they are out of chemical equilibrium with olivine, orthopyroxene, and spinel in the same sample). Finally, even if the NRM component held by sulfides in mantle peridotites is not well constrained, it is unlikely to be significant at mantle temperatures and pressures, where these phases would be in a liquid state.

9. Reason 8. Variations of magnetic properties of mantle xenoliths with tectonic setting

Details on magnetic methods are given in the Appendix A. Each xenolith sample yielded two 10-mm cubic specimens for magnetic analyses. Stepwise demagnetization of the natural remanent magnetization (NRM) was performed using alternating field up to 120 mT. The least altered specimens showed a single component of NRM and were kept for further tests. A few specimens' NRM demagnetization spectra displayed an additional high coercivity component, inferred to be carried by hematite, and were discarded because this mineral indicates that the specimen's original mineral assemblage was compromised by oxidation.

All mantle xenoliths show a relatively narrow range of magnetic susceptibilities and a broad range of NRM values (Fig. 4; Supplementary Data). The magnetic susceptibilities fit a log normal distribution

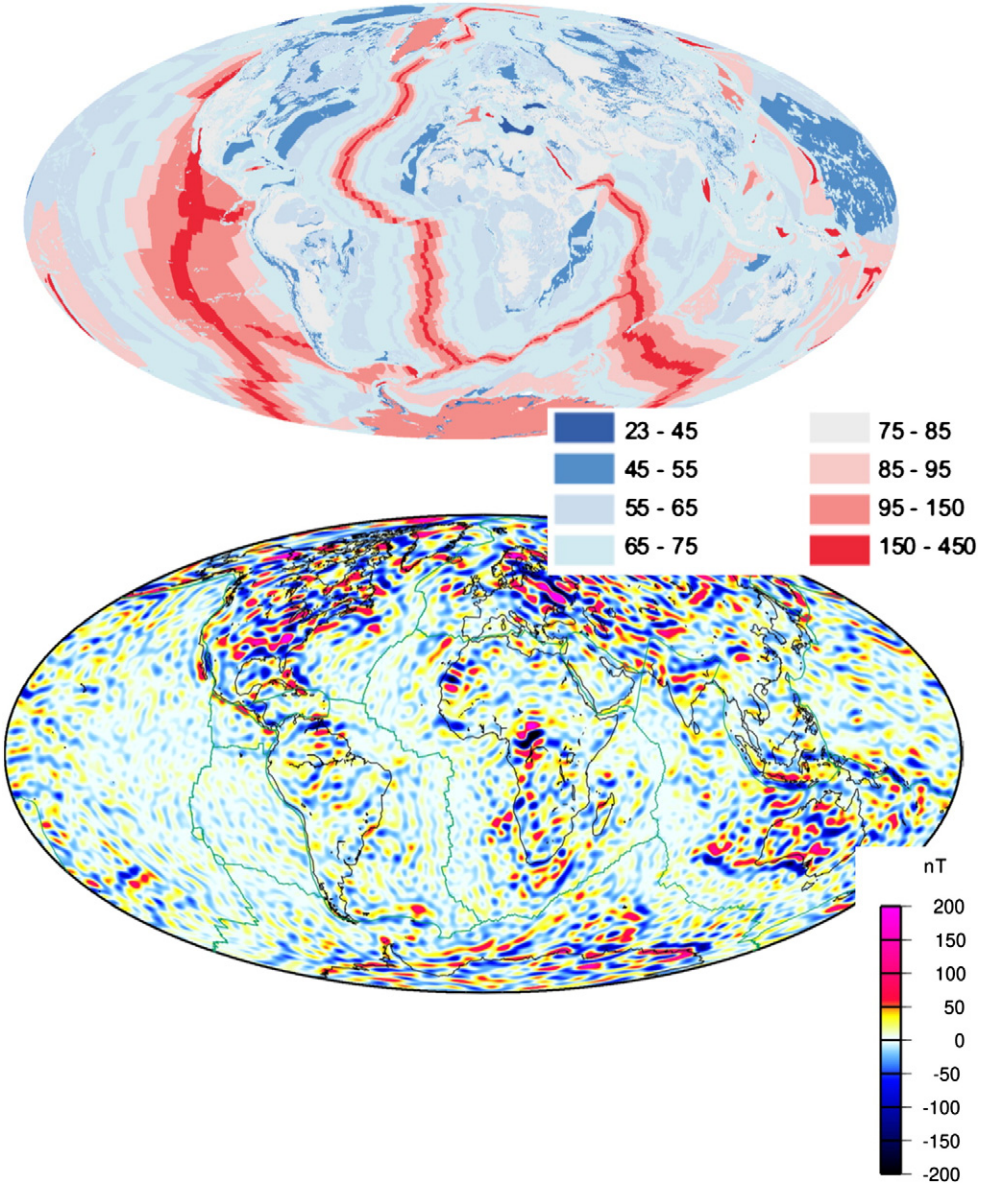

Fig. 8. The predicted geotherm in cratonic and forearc regions (A) can be relatively low. Detectable LWMA in these regions (B) may have an upper mantle component that has been up to now ignored in the inversion of magnetic observations.

(Supplementary Data). Low-field magnetic susceptibility (K_m) is a proxy for the concentration and grain size of ferromagnetic minerals, and to a lesser degree, the concentration of paramagnetic minerals. The NRM intensity of mantle xenoliths varies broadly between 10^{-4} and 1 A/m, and is an expression of the abundance of single domain and pseudo-single domain sized grains in a specimen, as well as the strength of the Earth's magnetic field at the time the magnetization was acquired. The Koenigsberger ratio (Q_n) represents the ratio of natural remanent magnetization to the induced magnetization in the Earth's field: $Q_n = \mathrm{NRM}/K_m\mathrm{H}$, where K_m is the magnetic susceptibility in SI units and H is the local geomagnetic field intensity (here 40 A/m). Values higher than 1 indicate that the specimen's remanent magnetization dominates the induced magnetization at ambient temperatures, while values less than 1 indicate that the specimen's induced magnetization is greater than the remanent magnetization. However, the measured remanent intensity at room temperature reflects the two-to-threefold increase in spontaneous magnetization of magnetite from the blocking temperature to room temperature, so the depth averaged in situ remanence at elevated temperatures (between the blocking temperature and the Curie point) is expected to be less than the measured NRM by a factor of 2–3 (Dunlop et al., 2010). Thus the depth averaged in situ remanence at elevated temperatures (between the blocking temperature and the Curie point) should be less than the measured NRM by a factor of 2–3. On the other hand, there is some enhancement of the susceptibility carried by SD magnetite above the blocking temperature, up to a factor of ~2 just below the Curie temperature. Dunlop et al. (2010) conclude that the expected Q values pertaining at elevated temperatures at depth range from ~0.2–0.3 for MD grains and ~1 for SD grains. Since the magnetic carrier in our xenolith samples is predominantly SD magnetite, the remanent and induced magnetizations at depth should be about equal. It is reasonable to assume that the remanence at depth is dominantly a viscous magnetization acquired during the Brunhes Chron, so the directions can be assumed to be consistent and approximately parallel to the induced magnetization, which means that the effect of remanence is to approximately double the magnetization that is calculated from measured susceptibilities.

Approximately one third of the xenoliths display Q_n values > 1, and if these specimens are representative of magnetic mineral assemblages in the lithospheric mantle, then these measurements suggest that the mantle's remanent magnetization may contribute to magnetic anomalies in low geotherm regions. Although there is a significant amount of overlap in the magnetic properties of xenoliths from different tectonic regions, we observe that, on average, specimens from the Siberian craton and Kamchatka island arc have higher NRM intensities than those from the Massif Central plume or the Hawai'i hot spot. Xenoliths from the subduction zone setting of the Kamchatka island arc have the highest Q_n values and their remanent magnetizations may play a more important role than their induced magnetizations in long wavelength magnetic anomalies.

The saturation magnetization normalized to mass (M_s) constitutes a proxy for the concentration of ferromagnetic minerals in the xenoliths. The ratio of the coercivity of remanence (H_{cr}) to the bulk coercivity (H_c) is directly related to the median magnetic domain grain size of a specimen's ferromagnetic minerals. Although the values of magnetic hysteresis parameters significantly overlap between suites, they plot in different regions of the M_s vs H_{cr}/H_c diagram (Ferré et al., 2013; Supplementary Data). The magnetic properties of fresh mantle xenoliths vary with tectonic setting (Fig. 4; Table) and also suggest that in cold geotherm regions, the uppermost mantle may contribute to LWMA anomalies (Fig. 8).

10. Conclusion

The view that "*the upper mantle is universally non-magnetic because it lacks ferromagnetic minerals and would be too hot to carry a magnetic remanence*" (Wasilewski and Mayhew, 1992; Wasilewski et al., 1979) has been challenged by new data on mantle xenoliths (Ferré et al., 2013). Until now, the source of LWMA was assumed to reside only in the lower crust. Evidence suggesting that the upper mantle may also contribute to magnetic anomalies is growing. Without additional information about magnetization of the mantle, differentiating these contributions from satellite or airborne data alone will remain difficult, even with spectral methods (e.g., Ravat et al., 2007). While deep crustal sources are currently examined, it is also crucial to re-evaluate the potential contribution of mantle rocks in various tectonic settings. We also believe that the non-magnetic mantle idea should be revisited because the forthcoming Swarm mission, to be launched in the Fall of 2013, will provide an unprecedented resolution of the lithospheric magnetic field.

Acknowledgments

We thank A. Tommasi and O. Alard for providing Hawai'i and Massif Central samples. D. Ionov acknowledges N. Pokhilenko (Novosibirsk Institute of Mineralogy), ALROSA for access to Udachnaya and collections, and CNRS PNP and PICS grants in 2010–2012. S.A.F. Thanks the Geological Society of America and the Institute for Rock Magnetism for support. We gratefully acknowledge the Guest Editor, Michael Purucker, and to the two reviewers, David Clark and Anonymous, for their insightful suggestions that help clarifying our views.

Appendix A

Magnetic measurements

Unoriented specimens were cut into 10 mm cubes using non-magnetic, diamond-impregnated blades from the center of xenoliths. Only specimens with one NRM component were included in Fig. 1. Two cubes were prepared from each specimen, and all specimens are free of basaltic glass. Low-field, room temperature, magnetic susceptibility was measured using a Kappabridge KLY-4S susceptometer at 875 Hz, 300 A/m; hysteresis properties were measured on a Princeton Measurements VSM 3900-04 at the Magnetic Laboratory at Southern Illinois University, Carbondale. NRMs were measured at the Institute for Rock Magnetism at the University of Minnesota, and at the paleomagnetic laboratories of the University of Madrid and the University of Burgos, using 2G Enterprises 760R and 755-1.65 three axis DC superconducting rock magnetometers respectively. Each sample was progressively AF demagnetized up to 170 mT.

Secondary electron microscopy

Samples were examined at the University of Minnesota's Characterization Facility using a thermally-assisted field emission gun JEOL 6500 scanning electron microscope outfitted with a Centaurus detector for backscattered imaging. Prior to imaging each sample was coated with a 50 Å thick layer of amorphous carbon to prevent charging. Samples were examined using an accelerating voltage of 15 kV and a working distance of 10.0 μm. Spot energy dispersive spectroscopy measurements and elemental line traverses were collected using a Thermo-Noran Vantage System. The diameter of the interaction volume for elemental measurements was 2.5 μm in silicate minerals and 2.0 μm in oxide and sulfide minerals. Matrix correction coefficients (Z, A, and F) were calculated using the Phi(Rho*z) method. X-ray spectra were collected using counting times of 60 s and a probe current of 100 nA.

Appendix B. Supplementary data

Supplementary data to this article can be found online at http://dx.doi.org/10.1016/j.tecto.2014.01.004.

References

Abercrombie, R.E., Ekström, G., 2001. Earthquake slip on oceanic transform faults. Nature 410 (6824), 74–77.

Alard, O., et al., 2011. Volatile-rich metasomatism in Montferrier xenoliths (Southern France): implications for the abundances of chalcophile and highly siderophile elements in the subcontinental mantle. J. Petrol. 52 (10), 2009–2045.

Alt, J.C., Shanks, W.C.I., 2003. Serpentinization of abyssal peridotites from the MARK area, Mid-Atlantic Ridge; sulfur geochemistry and reaction modeling. Geochim. Cosmochim. Acta 67 (4), 641–653.

Arkani-Hamed, J., 1993. The bulk magnetization contrast across the ocean–continent boundary in the east coast of North America. Geophys. J. Int. 115 (1), 152–158.

Arkani-Hamed, J., Strangway, D.W., 1986. Effective magnetic susceptibility of the oceanic upper mantle derived from Magsat data. Geophys. Res. Lett. 13 (10), 999–1002.

Arkani-Hamed, J., Strangway, D.W., 1987. An interpretation of magnetic signatures of subduction zones detected by MAGSAT. Tectonophysics 133 (1–2), 45–55.

Arnaiz-Rodriguez, M.S., Orihuela, N., 2013. Curie point depth in Venezuela and the Eastern Caribbean. Tectonophysics 590, 38–51.

Ashworth, J.R., Chambers, A.D., 2000. Symplectic Reaction in Olivine and the Controls of Intergrowth Spacing in Symplectites. J. Petrol. 41 (2), 285–304.

Ballhaus, C., Berry, R., Green, D., 1991. High pressure experimental calibration of the olivine–orthopyroxene–spinel oxygen geobarometer: implications for the oxidation state of the upper mantle. Contrib. Mineral. Petrol. 107 (1), 27–40.

Ballhaus, C., Berry, R.F., Green, D.H., 1990. Oxygen fugacity controls in the Earth's upper mantle. Nature 348 (6300), 437–440.

Barnes, S., 2001. The range of spinel compositions in terrestrial mafic and ultramafic rocks. J. Petrol. 42 (12), 2279–2302.

Batumike, J.M., Griffin, W.L., O'Reilly, S.Y., 2009. Lithospheric mantle structure and the diamond potential of kimberlites in southern D.R. Congo. Lithos 112, Suppl. 1(0), 166–176.

Belley, F., Ferré, E.C., Martín-Hernández, F., Jackson, M.J., Dyar, M.D., Catlos, E.J., 2009. The magnetic properties of natural and synthetic $(Fe_x, Mg_{1-x})_2 SiO_4$ olivines. Earth Planet. Sci. Lett.. http://dx.doi.org/10.1016/j.epsl.2009.05.016.

Blackwell, D., et al., 2011. Temperature at depth maps for the conterminous US and geothermal resource estimates. Geotherm. Resour. Counc. Trans. 35.

Blakely, R.J., Brocher, T.M., Wells, R.E., 2005. Subduction-zone magnetic anomalies and implications for hydrated forearc mantle. Geology 33 (6), 445–448.

Bleil, U., Pertersen, N., 1982. Physical properties of rocks. In: Angenheister, G. (Ed.), Landolt-Bornstein numerical data and functional relationships in Science and Technology; Group V. Geophysics and Space Research, vol. 1b. Springer-Verlab, New York, pp. 308–432.

Borradaile, G.J., Lagroix, F., 2001. Magnetic fabrics reveal upper mantle flow fabrics in the Troodos ophiolite complex, Cyprus. J. Struct. Geol. 23 (8), 1299–1317.

Bostock, M.G., Hyndman, R.D., Rondenay, S., Peacock, S.M., 2002. An inverted continental Moho and serpentinization of the forearc mantle. Nature 417, 536–538.

Brewster, D., O'Reilly, W., 1988. Magnetic properties of synthetc analogues of the altered olivines of igneous rocks. Geophys. J. 95, 421–432.

Bronner, A., Sauter, D., Manatschal, G., Peron-Pinvidic, G., Munschy, M., 2011. Magmatic breakup as an explanation for magnetic anomalies at magma-poor rifted margins. Nat. Geosci. 4 (8), 549–553.

Bussod, G.Y.A., Williams, D.R., 1991. Thermal and kinematic model of the southern Rio Grande rift: inferences from crustal and mantle xenoliths from Kilbourne Hole, New Mexico. Tectonophysics 197 (2–4), 373–389.

Callahan, C.N., 2009. Magnetic properties of unaltered and metasomatized mantle xenoliths from the Rio Puerco volcanic necks, NM. University of New Mexico, Albuquerque, NM.

Carlson, R.W., 2007. The mantle and core. Treatise on GeochemistryElsevier 2.

Chakraborty, S., 1997. Rates and mechanisms of Fe–Mg interdiffusion in olivine at 980°–1300 °C. J. Geophys. Res. Solid Earth 102 (B6), 12317–12331.

Chiozzi, P., Matsushima, J., Okubo, Y., Pasquale, V., Verdoya, M., 2005. Curie-point depth from spectral analysis of magnetic data in central-southern Europe. Phys. Earth Planet. Inter. 152 (4), 267–276.

Christensen, N.I., 1971. Fabric, seismic anisotropy, and tectonic history of the Twin Sisters dunite, Washington. Geol. Soc. Am. Bull. 82, 1681–1694.

Clark, D.A., 1999. Magnetic petrology of igneous intrusions: implications for exploration and magnetic interpretation. Explor. Geophys. 30 (2), 5–26.

Costa, F., Chakraborty, S., 2008. The effect of water on Si and O diffusion rates in olivine and implications for transport properties and processes in the upper mantle. Phys. Earth Planet. Inter. 166, 11–29.

Counil, J.-L., Achache, J., Galdeano, A., 1989. Long-wavelength magnetic anomalies in the Caribbean: plate boundaries and allochthonous continental blocks. J. Geophys. Res. Solid Earth 94 (B6), 7419–7431.

Creighton, S., Stachel, T., Eichenberg, D., Luth, R., 2010. Oxidation state of the lithospheric mantle beneath Diavik diamond mine, central Slave craton, NWT, Canada. Contrib. Mineral. Petrol. 159 (5), 645–657.

Dahlin, D.C., Rule, A.R., 1993. Magnetic susceptibility of minerals in high magnetic fields. United States Department of the Interior, Bureau of Mines (13 p).

Davies, J.H., Davies, D.R., 2010. Earth's surface heat flux. Solid Earth 1 (1), 5–24.

Dekkers, M.J., 1988. Magnetic properties of natural pyrrhotite part I: behaviour of initial susceptibility and saturation-magnetization-related rock-magnetic parameters in a grain-size dependent framework. Phys. Earth Planet. Inter. 52, 376–393.

Demouchy, S., Jacobsen, S.D., Gaillard, F., Stern, C.R., 2006. Rapid magma ascent recorded by water diffusion profiles in mantle olivine. Geology 34 (6), 429–432.

Derbyshire, W.D., Yearian, H.J., 1958. X-ray diffraction and magnetic measurements of the Fe–Cr spinels. Phys. Rev. 112 (5), 1603–1607.

Deschamps, F., et al., 2010. In situ characterization of serpentinites from forearc mantle wedges: timing of serpentinization and behavior of fluid-mobile elements in subduction zones. Chem. Geol. 269 (3,Äì), 262–277.

Dohmen, R., Chakraborty, S., 2007. Fe-Mg diffusion in olivine II: point defect chemistry, change of diffusion mechanisms and a model for calculation of diffusion coefficients in natural olivine. Phys. Chem. Miner. 34 (6), 409–430.

Doucet, L.S., Ionov, D.A., Golovin, A.V., Pokhilenko, N.P., 2012. Depth, degrees and tectonic settings of mantle melting during craton formation: inferences from major and trace element compositions of spinel harzburgite xenoliths from the Udachnaya kimberlite, central Siberia. Earth Planet. Sci. Lett. 359–360, 206–218.

Dromgoole, E.L., Pasteris, J.D., 1987. Interpretation of the sulfide assemblages in a suite of xenoliths from Kilbourne Hole, New Mexico. Geol. Soc. Am. Spec. Pap. 215, 25–46.

Drury, M.R., van Roermund, H.L.M., 1989. Reply to comment by R.L. Hervig on "Metasomatic origin for Fe–Ti-rich multiphase inclusions in olivine from kimberlite xenoliths". Geology 17 (7), 676–677.

Dunlop, D.J., Özdemir, Ö., Costanzo-Alvarez, V., 2010. Magnetic properties of rocks of the Kapuskasing uplift (Ontario, Canada) and origin of long-wavelength magnetic anomalies. Geophys. J. Int. 183 (2), 645–658.

Dunlop, D.J., Özdemir, Ö., 1997. Rock magnetism: fundamentals and frontiers. Cambridge Studies in Magnetism. Cambridge University Press, Cambridge (573 p).

Dunlop, D.J., Ozdemir, O., 2009. Magnetizations in Rocks and Minerals. In: Kono, M. (Ed.), Geomagnetism. Elsevier, Amsterdam, pp. 277–336.

Dyment, J., Arkani-Hamed, J., Ghods, A., 1997. Contribution of serpentinized ultramafics to marine magnetic anomalies at slow and intermediate spreading centers: insights from the shape of the anomalies. Geophys. J. Int. 129 (3), 691–701.

Ernst, W.G., 1988. Tectonic history of subduction zones inferred from retrograde blueschist P–T paths. Geology 16 (12), 1081–1084.

Facer, J., Downes, H., Beard, A., 2009. In situ serpentinization and hydrous fluid metasomatism in spinel dunite xenoliths from the Bearpaw Mountains, Montana, USA. J. Petrol. 50 (8), 1443–1475.

Ferré, E.C., et al., 2013. The magnetism of mantle xenoliths and potential implications for sub-Moho magnetic sources. Geophys. Res. Lett. 40 (1–6). http://dx.doi.org/10.1029/2012GL054100.

Ferré, E.C., Tikoff, B., Jackson, M., 2005. The magnetic anisotropy of mantle peridotites: example from the Twin Sisters dunite, Washington. Tectonophysics 398 (3–4), 141–166.

Fleet, M.L., Bilcox, G.A., Barnett, R.L., 1980. Oriented magnetite inclusions in pyroxenes from the Grenville Province. Can. Mineral. 18, 89–99.

Foley, S.F., 2011. A reappraisal of redox melting in the Earth's mantle as a function of tectonic setting and time. J. Petrol. 52 (7–8), 1363–1391.

Franz, L., Wirth, R., 2000. Spinel inclusions in olivine of peridotite xenoliths from TUBAF seamount (Bismarck Archipelago/Papua New Guinea): evidence for the thermal and tectonic evolution of the oceanic lithosphere. Contrib. Mineral. Petrol. 140 (3), 283–295.

Frey, F.A., Prinz, M., 1978. Ultramafic inclusions from San Carlos, Arizona: Petrologic and geochemical data bearing on their petrogenesis. Earth Planet. Sci. Lett. 38 (1), 129–176.

Friedman, S.A., 2011. Magnetic Properties of Mantle Xenoliths and Implications for Long Wavelength Anomalies. Southern Illinois University, Carbondale (91 pp.).

Friedman, S.A., Feinberg, J.M., Ferré, E.C., Demory, F., Martín-Hernández, F., Conder, J.A., Rochette, P., 2014. Cratons vs. rift uppermost mantle contributions to magnetic anomalies in the United States interior. Tectonophysics. 624–625, 15–23 (this issue).

Frost, B.R., 1985. On the stability of sulfides, oxides, and native metals in serpentinite. J. Petrol. 26 (1), 31–63.

Frost, B.R., Evans, K., Swapp, S.M., Beard, J.S., Mothersole, F.E., 2013. The process of serpentinization in dunite from New Caledonia. Lithos 178, 24–39.

Frost, B.R., Shive, P.N., 1989. Comment on "Limiting depth of magnetization in cratonic lithosphere". Geophys. Res. Lett. 16 (5), 477–479.

Frost, D.J., McCammon, C.A., 2008. The redox state of Earth's mantle. Annu. Rev. Earth Planet. Sci. 36 (1), 389–420.

Gattacceca, J., Rochette, P., Lagroix, F., Mathé, P.E., Zanda, B., 2011. Low temperature magnetic transition of chromite in ordinary chondrites. Geophys. Res. Lett. 38 (10), L10203.

Goncharov, A.G., Ionov, D.A., Doucet, L.S., 2012. Thermal state, oxygen fugacity and C–O–H fluid speciation in cratonic lithospheric mantle. New data on peridotite xenoliths from the Udachnaya kimberlite, Siberia. Earth Planet. Sci. Lett. http://dx.doi.org/10.1016/j.epsl.2012.09.016.

Griffin, W.L., et al., 2011. Archean lithospheric mantle beneath Arkansas: continental growth by microcontinent accretion. Geol. Soc. Am. Bull. 123 (9–10), 1763–1775.

Guevara, N.O., Garcia, A., Arnaiz, M., 2013. Magnetic anomalies in the Eastern Caribbean. Int. J. Earth Sci. 102 (3), 591–604.

Haggerty, S.E., 1995. Upper mantle mineralogy. J. Geodyn. 20 (4), 331–364.

Haggerty, S.E., Sautter, V., 1990. Ultradeep (greater than 300 km), ultramafic upper mantle xenoliths. Science 248 (4958), 993–996.

Harrison, C.G.A., Carle, H.M., 1981. Intermediate wavelength magnetic anomalies over ocean basins. J. Geophys. Res. 86 (B12), 11585–11599.

Hemant, K., Maus, S., 2005a. Geological modeling of the new CHAMP magnetic anomaly maps using a geographical information system technique. J. Geophys. Res. Solid Earth 110.

Hemant, K., Maus, S., 2005b. Why no anomaly is visible over most of the continent–ocean boundary in the global crustal magnetic field. Phys. Earth Planet. Inter. 149 (3–4), 321–333.

Hervig, R.L., 1989. Comment on "Metasomatic origin for Fe–Ti-rich multiphase inclusions in olivine from kimberlite xenoliths". Geology 17 (7), 675–676.

Hofer, H.E., Lazarov, M., Brey, G.P., Woodland, A.B., 2009. Oxygen fugacity of the metasomatizing melt in a polymict peridotite from Kimberley. Lithos 112, Supplement 2(0), 1150–1154.

Hwang, S.-L., et al., 2008. Hematite and magnetite precipitates in olivine from the Sulu peridotite: a result of dehydrogenation-oxidation reaction of mantle olivine? Am. Mineral. 93 (7), 1051–1060.
Ildefonse, B., September 2010. The MoHole: a crustal journey and mantle quest, workshop in Kanazawa, Japan, 3–5 June 2010. Sci. Drill. 10, 56–63.
Ionov, D.A., 2010. Petrology of mantle wedge lithosphere: new data on supra-subduction zone peridotite xenoliths from the Andesitic Avacha Volcano, Kamchatka. J. Petrol. 51 (1–2), 327–361.
Ionov, D.A., Benard, A., Plechov, P.Y., 2011. Melt evolution in subarc mantle: evidence from heating experiments on spinel-hosted melt inclusions in peridotite xenoliths from the andesitic Avacha volcano (Kamchatka, Russia). Contrib. Mineral. Petrol. 162, 1159–1174.
Ionov, D.A., Doucet, L.S., Ashchepkov, I.V., 2010. Composition of the lithospheric mantle in the Siberian craton: new constraints from fresh peridotites in the Udachnaya-East Kimberlite. J. Petrol. 51 (11), 2177–2210.
Irvine, T.N., 1965. Chromian spinel as a petrogenetic indicator. I. Theory. Can. J. Earth Sci. 2, 648–672.
Irvine, T.N., 1967. Chromian spinel as a petrogenetic indicator. II. Petrologic applications. Can. J. Earth Sci. 4, 71–103.
Irving, A.J., 1980. Petrology and geochemistry of composite ultramafic xenoliths in alkalic basalts and implications for magmatic processes within the mantle. Am. J. Sci. 280-A, 389–426.
Ishimaru, S., Arai, S., Shukuno, H., 2009. Metal-saturated peridotite in the mantle wedge inferred from metal-bearing peridotite xenoliths from Avacha volcano, Kamchatka. Earth Planet. Sci. Lett. 284 (3–4), 352–360.
Jackson, I., 1998. The Earth's Mantle. Cambridge University Press.
Janecky, D.R., Seyfried Jr., W.E., 1986. Hydrothermal serpentinization of peridotite within the oceanic crust: experimental investigations of mineralogy and major element chemistry. Geochim. Cosmochim. Acta 50 (7), 1357–1378.
Jones, A.G., Carlson, R.W., Grütter, H., 2003. The Slave–Kaapvaal workshop: a tale of two cratons. Lithos 71 (2-4), ix–xi.
Kądziałko-Hofmokl, M., Delura, K., Bylina, P., Jeleńska, M., Kruczyk, J., 2008. Mineralogy and magnetism of Fe–Cr spinel series minerals from podiform chromitites and dunites from Tąpadła (Sudetic ophiolite, SW Poland) and their relationship to palaeomagnetic results of the dunites. Geophys. J. Int. 175 (3), 885–900.
Kinman, W.S., Neal, C.R., 2006. Magma evolution revealed by anorthite-rich plagioclase cumulate xenoliths from the Ontong Java Plateau: insights into LIP magma dynamics and melt evolution. J. Volcanol. Geotherm. Res. 154 (1,Äi2), 131–157.
Knop, O., Huang, C.-H., Reid, K.I.G., Carlow, J.S., Woodhams, F.W.D., 1976. Chalkogenides of the transition elements. X. X-ray, neutron, Mössbauer, and magnetic studies of pentlandite and the π phases π (Fe, Co, Ni, S), Co8MS8, and Fe4Ni4MS8 (M = Ru, Rh, Pd). J. Solid State Chem. 16 (1–2), 97–116.
Kobussen, A.F., Griffin, W.L., O'Reilly, S.Y., Shee, S.R., 2008. Ghosts of lithospheres past: imaging an evolving lithospheric mantle in southern Africa. Geology 36 (7), 515–518.
Kochemasov, G.G., Chuprov, A.I., 1990. The Bangui magnetic anomaly in Central Africa in the light of new geological evidence. Int. Geol. Rev. 32 (2), 151–161.
Kohlstedt, D.L., Goetze, C., Durham, W.B., Sande, J.V., 1976. New technique for decorating dislocations in Olivine. Science 191 (4231), 1045–1046.
Lenoir, X., Garrido, C.J., Bodinier, J.-L., Dautria, J.-M., 2000. Contrasting lithospheric mantle domains beneath the Massif Central (France) revealed by geochemistry of peridotite xenoliths. Earth Planet. Sci. Lett. 181 (3), 359–375.
Le Roux, V., et al., 2007. The Lherz spinel lherzolite: refertilized rather than pristine mantle. Earth Planet. Sci. Lett. 259 (3–4), 599–612.
Li, Z.-X.A., Lee, C.-T.A., Peslier, A.H., Lenardic, A., Mackwell, S.J., 2008. Water contents in mantle xenoliths from the Colorado Plateau and vicinity: implications for the mantle rheology and hydration-induced thinning of continental lithosphere. J. Geophys. Res. Solid Earth 113 (B9), B09210.
Liou, J.G., 1999. Petrotectonic summary of less-intensively studied UHP regions. Int. Geol. Rev. 41, 571–586.
Liou, J.G., Zhang, R.Y., Ernst, W.G., 2007. Very high-pressure orogenic garnet peridotites. Proc. Natl. Acad. Sci. 104 (22), 9116–9121.
Luguet, A., Lorand, J.-P., 1998. Altération supergène et teneurs en soufre des xénolithes du manteau: Une approche à partir des Iherzolites des basaltes de Montferrier (Languedoc, France). C. R. Acad. Sci. IIA Earth Planet. Sci. 327 (8), 519–525.
MacGregor, I.D., 1970. The effect of CaO, Cr2O3, Fe2O3 and Al2O3 on the stability of spinel and garnet peridotites. Phys. Earth Planet. Inter. 3, 372–377.
MacGregor, I.D., 1974. The system MgO–Al2O3–SiO2: solubility of Al2O3 in enstatite for spinel and garnet peridotite compositions. Am. Mineral. 59, 110–119.
Mackwell, S.J., 1992. Oxidation kinetics of fayalite (Fe2SiO4). Phys. Chem. Miner. 19, 220–228.
Malvoisin, B., Carlut, J., Brunet, F., 2012. Serpentinization of oceanic peridotites: 1. A high-sensitivity method to monitor magnetite production in hydrothermal experiments. J. Geophys. Res. 117 (B1), B01104.
Manea, V.C., Perez-Gussinye, M., Manea, M., 2012. Chilean flat slab subduction controlled by overriding plate thickness and trench rollback. Geology 40 (1), 35–38.
Markl, G., Marks, M., Wirth, R., 2001. The influence of T, a SiO2, and fO2 on exsolution textures in Fe–Mg olivine: an example from augite syenites of the Ilimaussaq Intrusion, South Greenland. Am. Mineral. 86, 36–46.
Mattioli, G.S., Wood, B.J., 1986. Upper mantle oxygen fugacity recorded by spinel lherzolites. Nature 322 (6080), 626–628.
Maus, S., et al., 2006. Earth's lithospheric magnetic field determined to spherical harmonic degree 90 from CHAMP satellite measurements. Geophys. J. Int. 164 (2), 319–330.
McCammon, C., Kopylova, M.G., 2004. A redox profile of the Slave mantle and oxygen fugacity control in the cratonic mantle. Contrib. Mineral. Petrol. 148 (1), 55–68.
McEnroe, S.A., Brown, L.L., 2000. A closer look at remanence-dominated aeromagnetic anomalies: rock magnetic properties and magnetic mineralogy of the Russel Belt monocline-sillimanite–gneiss, northwest Adirondack Mountains, New York. J. Geophys. Res. 105, 16,437–16,456.
McKenzie, D., Jackson, J., Priestley, K., 2005. Thermal structure of oceanic and continental lithosphere. Earth Planet. Sci. Lett. 233, 337–349.
Moseley, D., 1984. Symplectic exsolution in olivine. Am. Mineral. 69, 139–153.
Moskowitz, B.M., 1991. Hitchhiker's Guide to Magnetism. University of Minnesota, Minneapolis (48 p).
Nazarova, K.A., 1994. Serpentinized peridotites as a possible source for oceanic magnetic anomalies. Mar. Geophys. Res. 16, 455–462.
Neal, C.R., Haggerty, S.E., Sautter, V., 2001. "Majorite" and "Silicate Perovskite" mineral Compositions in xenoliths from Malaita. Science 292 (5519), 1015-1015.
Neal, C.R., Nixon, P.H., 1985. Spinel–garnet relationships in mantle xenoliths from the Malaita alnoeites, Solomon Islands, south-western Pacific. S. Afr. J. Geol. 88, 347–354.
Nicolas, A., 1986. Structure and petrology of peridotites: clues to their environment. Rev. Geophys. 24, 875–895.
Nitsan, U., 1974. Stability field of olivine with respect to oxidation and reduction. J. Geophys. Res. 79 (5), 706–711.
Nixon, P.H., 1987. Mantle Xenoliths. John Wiley & Sons, Chichester (844 pp.).
Ouabego, M., et al., 2013. Rock magnetic investigation of possible sources of the Bangui magnetic anomaly. Phys. Earth Planet. Inter. 224, 11–20.
Peslier, A.H., Woodland, A.B., Wolff, J.A., 2008. Fast kimberlite ascent rates estimated from hydrogen diffusion profiles in xenolithic mantle olivines from southern Africa. Geochim. Cosmochim. Acta 72 (11), 2711–2722.
Pollack, H.N., Chapman, D.S., 1977. Mantle heat flow. Earth Planet. Sci. Lett. 34, 174–184.
Popov, K.V., Bazylev, B.A., Shcherbakov, V.P., Gapeev, A.K., 2011. Comparison between the magnetic and petrological characteristics of the peridotites from the Gorringe ridge and the peridotites from the mid-ocean ridges. Oceanology 51 (1), 157–169.
Puga, E., Cruz, M.D.R., De Frederico, A.D., 1999. Magnetite–silicate inclusions in olivine of ophiolitic metagabbros from the Mulhacén Complex, Betic Cordillera, Southeastern Spain. Can. Mineral. 37, 1191–1209.
Purucker, M., Clark, D., 2011. Mapping and interpretation of the lithospheric magnetic field, geomagnetic observations and models. IAGA Special Sopron Book Series. Springer, Netherlands 311–337.
Putnis, A., 1979. Electron petrography of high-temperature oxidation in olivine from the Rhum layered intrusion. Mineral. Mag. 43, 293–296.
Quintiliani, M., Andreozzi, G.B., Graziani, G., 2006. Fe2+ and Fe3+ quantification by different approaches and fO2 estimation for Albanian Cr-spinels. Am. Mineral. 91, 907–916.
Rais, A., et al., 2003. Cation distribution and magnetic properties of natural chromites. Phys. Status Solidi B 239 (2), 439–446.
Rais, A., Yousif, A.A., Worthing, M.A., Al-Alawi, Z., 1997. Magnetic susceptibilities of chromites from Oman. Mineral. Mag. 61, 726–728.
Ravat, D., 2012. North American magnetic bottom/Curie depth estimates and their significance for lithospheric temperatures and magnetization. 2012 Fall Meeting, AGU, San Francisco, Calif., 3–7 Dec, p. GP13C-06.
Ravat, D., Pignatelli, A., Nicolosi, I., Chiappini, M., 2007. A study of spectral methods of estimating the depth to the bottom of magnetic sources from near-surface magnetic anomaly data. Geophys. J. Int. 169 (2), 421–434.
Ravat, D., Salem, A., Abdelaziz, A.M.S., Elawadi, E., Morgan, P., 2011. Probing magnetic bottom and crustal temperature variations along the Red Sea margin of Egypt. Tectonophysics 510 (3–4), 337–344.
Raye, U., et al., 2011. Composition of the mantle lithosphere beneath south-central Laurentia: Evidence from peridotite xenoliths, Knippa, Texas. Geosphere 7 (3), 710–723.
Rhodes, J.M., Vollinger, M.J., 2005. Ferric/ferrous ratios in 1984 Mauna Loa lavas: a contribution to understanding the oxidation state of Hawaiian magmas. Contrib. Mineral. Petrol. 149 (6), 666–674.
Rochette, P., Fillion, G., Mattéi, J.-L., Dekkers, M.J., 1990. Magnetic transition at 30–34 K in pyrrhotite: insight into a widespread occurrence of this mineral in rocks. Earth Planet. Sci. Lett. 98 (3–4), 319–328.
Schlinger, C.M., Veblen, D.R., 1989. Magnetism and transmission electron microscopy of Fe–Ti oxides and pyroxenes in a granulite from Lofoten, Norway. J. Geophys. Res. Solid Earth 94 (B10), 14009–14026.
Schmidbauer, E., 1983. Magnetization of Fe–Cr–Ti spinels. Phys. Chem. Miner. 9 (3), 124–126.
Sen, G., Jones, R.E., 1988. Exsolved silicate and oxide phases from clinopyroxenes in a single Hawaiian xenolith: Implications for oxidation state of the Hawaiian upper mantle. Geology 16 (1), 69–72.
Shive, P.N., 1989. Can remanent magnetization in the deep crust contribute to long wavelength magnetic anomalies? Geophys. Res. Lett. 16 (1), 89–92.
Soustelle, V., Tommasi, A., Demouchy, S., Ionov, D.A., 2010. Deformation and fluid–rock interaction in the supra-subduction mantle: Microstructures and water contents in peridotite xenoliths from the Avacha Volcano, Kamchatka. J. Petrol. 51 (1–2), 363–394.
Syono, Y., 1960. Magnetic susceptibility of some rock forming silicate minerals such as amphiboles, biotites, cordierites and garnets. J. Geomagn. Geoelectr. 11, 85–93.
Tarling, D.H., Hrouda, F., 1993. The magnetic anisotropy of rocks. Chapman & Hall, London (217 p).
Taylor, L.A., Neal, C.R., 1989. Eclogites with crustal and mantle signatures from the Bellsbank kimberlite, South Africa, part 1: mineralogy, petrography, and whole-rock geochemistry. J. Geol. 97, 551–567.
Thebault, E., Purucker, M., Whaler, K.A., Langlais, B., Sabaka, T.J., 2010. The magnetic field of the Earth's lithosphere. Space Sci. Rev. 155, 95–127.
Thompson, G.A., Robinson, R., 1975. Gravity and magnetic investigation of the Twin Sisters dunite, Northern Washington. Geol. Soc. Am. Bull. 86 (10).

Toft, P.B., Arkani-Hamed, J., Haggerty, S.E., 1990. The effects of serpentinization on density and magnetic susceptibility; a petrophysical model. Phys. Earth Planet. Inter. 65 (1–2), 137–157.
Toft, P.B., Haggerty, S.E., 1988. Limiting depth of magnetization in cratonic lithosphere. Geophys. Res. Lett. 15 (5), 530–533.
Tsujimori, T., Sisson, V.B., Liou, J.G., Harlow, G.E., Sorensen, S.S., 2006. Very-low-temperature record of the subduction process: a review of worldwide lawsonite eclogites. Lithos 92 (3–4), 609–624.
Walz, F., 2002. The Verwey transition — a topical review. J. Phys. Condens. Matter 14 (12), 285–340.
Warner, R.D., Wasilewski, P.J., 1995. Magnetic petrology of lower crust and upper mantle xenoliths from McMurdo Sound, Antarctica. Tectonophysics 249 (1–2), 69–92.
Wasilewski, P.J., 1987. Magnetic properties of mantle xenoliths and the magnetic character of the crust–mantle boundary. In: Nixon, P.H. (Ed.), Mantle Xenoliths. John Wiley and Sons Ltd., London, pp. 577–588.
Wasilewski, P., 1988. A new class of natural magnetic materials: the ordering alloys. Geophys. Res. Lett. 15 (5), 534–537.
Wasilewski, P.J., Mayhew, M.A., 1992. The Moho as a magnetic boundary revisited. Geophys. Res. Lett. 19 (22), 2259–2262.
Wasilewski, P.J., Thomas, H.H., Mayhew, M.A., 1979. The Moho as a magnetic boundary. Geophys. Res. Lett. 6, 541–544.
Williams, M.C., et al., 1985. Magnetic properties of exposed deep crustal rocks from the Superior Province of Manitoba. Earth Planet. Sci. Lett. 76 (1–2), 176–184.
Wood, B.J., 1991. Oxygen barometry of spinel peridotites. Rev. Mineral. Geochem. 25 (1), 417–432.
Wood, B.J., Bryndzia, L.T., Johnson, K.E., 1990. Mantle oxidation state and its relationship to tectonic environment and fluid speciation. Science 248 (4953), 337–345.
Woodland, A.B., Koch, M., 2003. Variation in oxygen fugacity with depth in the upper mantle beneath the Kaapvaal craton, Southern Africa. Earth Planet. Sci. Lett. 214 (1–2), 295–310.
Young, H.P., Lee, C.T.A., 2009. Fluid-metasomatized mantle beneath the Ouachita belt of southern Laurentia: Fate of lithospheric mantle in a continental orogenic belt. Lithosphere 1 (6), 370–383.
Yu, Y., Tikoff, B., 2010. Magnetism of Cr-rich spinel, American Geophysical Union Fall Meeting, GP43A-1037, San Francisco, CA.
Zhang, R.Y., Shu, J.F., Mao, H.K., Liou, J.G., 1999. Magnetite lamellae in olivine and clinohumite from Dabie UHP ultramafic rocks, central China. Am. Mineral. 84, 564–569.
Zhao, D., Essene, E.J., Zhang, Y., 1999. An oxygen barometer for rutile–ilmenite assemblages: oxidation state of metasomatic agents in the mantle. Earth Planet. Sci. Lett. 166 (3–4), 127–137.
Ziemniak, S.E., Castelli, R.A., 2003. Immiscibility in the Fe3O4–FeCr2O4 spinel binary. J. Phys. Chem. Solids 64 (11), 2081–2091.